I S A V

Journal of Theoretical and Applied

Vibration and Acoustics

journal homepage: http://tava.isav.ir

Free vibration and aeroelastic analyses of rectangular cantilever plates including correlation with experiment

AmirHossein Modaress-Aval[a], Firooz Bakhtiari-Nejad[a*], Hamidreza Rostami[a], Earl H. Dowell[b]

[a] *Amirkabir University of Technology, Tehran, Iran*

[b] *Duke University, Durham, NC, USA*

ARTICLE INFO

Article history:
Received 26 February 2020

Received in revised form
5 May 2020

Accepted 3 June 2020

Available online 8 June 2020

Keywords:
Rayleigh-Ritz method,

Rectangular cantilever plates,

Classical plate theory,

Aeroelasticity,

Flutter.

ABSTRACT

In the present study, the free vibration and aeroelastic problems of rectangular cantilever plates with varying aspect ratio have been investigated. The classical plate theories based on the Kirchhoff hypothesis have been adopted to simulate the structural response of the plate. The Peter's theory is selected to model the aerodynamic pressure on the plate due to the incompressible air flow. To discretize the partial deferential equations of the system, the Rayleigh-Ritz method has been applied and by using Lagrange equations, the mass, damping, and stiffness matrices have been derived. Various numbers of mode shapes are used to show the convergence of the response of the system . The theoretical results including the natural frequencies and flutter speed have been evaluated by using the experimental data obtained from the ground vibration experiment carried out at Duke University. It has been shown that for a relatively low aspect ratio rectangular cantilever plate, using some techniques in Rayleigh–Ritz method leads to an improvement of the results for both the natural frequencies and flutter speed. This technique ends up having two sets of decoupled equations and consequently, the number of equations that have to be solved simultaneously is divided by two. This could lead to a reduction of computational time significantly.

1. Introduction

In the design of aerospace structures, a rectangular cantilever plate is frequently used as a simple model to capture the structural response of different parts. Thus, the free vibration and

* Corresponding author:
E-mail address: f_b_nejad@yahoo.com (F. Bakhtiari-Nejad)

http://dx.doi.org/ 10.22064/tava.2021.121930.1157

aeroelastic analyses of thin rectangular cantilever plates is a subject that has received the attention of numerous researchers throughout the past century.

Among different theories, the Euler–Bernoulli beam theory and the classical plate theory have been applied more than others. For high aspect ratios (AR>10) rectangular plates, the beam theory is the first choice in analyses. While, for low aspect ratio rectangular plates, the classic plate theory has been mainly selected by investigators to model the structural response of the system.

In the Euler–Bernoulli beam theory, a closed-form solution of the partial differential equations governing the free vibrations is possible. In contrast, there is no exact closed-form solution for the problems concerning the free vibrations of rectangular cantilever plates with the use of the classical plate theory. The absence of such exact solutions necessitates the investigation for approximate solutions. The solution methods for these problems include analytical, semi-analytical-numerical, and numerical methods. In this regard, this work presents only an overview of the use of different solution methods in the study of the free vibrations of plates.

For the solution of free vibration, static, and buckling problems of rectangular cantilever plates, the Rayleigh, the Rayleigh-Ritz, and the Kantorovich methods have been primarily used for several decades in comparison to other analytical and numerical methods. The most significant study in the classical literature (up to 1990) on plate vibration and solution methods is the masterful book by Leissa1[1].

During the last two decades, researchers have mostly concentrated on more complicated problems in the analysis of plates such as taking composite material and orthotropic behaviour into accounting in addition to considering shear deformable theories for thick plates or nonhomogeneous boundary conditions. In this study, however, we have mainly concentrated on those studies investigating the free vibration analysis of an isotropic thin rectangular cantilever plate.

Shen *et.al* (2003) conducted an analytical study to determine the characteristics associated with the vibrations of a strengthened plate with various boundary conditions. They used a set of beam Eigen functions, which satisfies geometric boundary conditions. They also adopted the Rayleigh-Ritz method with the set of admissible functions to calculate the deflections, stresses, and natural frequencies of the plate [2] Seok *et.al* (2004) studied the free vibrations of rectangular cantilever plates considering only the out of plane motion using a variational approximation procedure. They demonstrated that the results are compatible with those obtained from FEM, and therefore, show the accuracy of this procedure [3]. Next, they did a similar study considering only the in-plane motion[4] Wang and Xu (2010) analyzed the free vibration of annular plates, rectangular plates, and beams, under free boundary conditions with the use of the discrete singular convolution. They introduced a novel method applicable to the free boundary conditions. They proved that this method is simple to use and can lead to accurate theoretical frequency obtained for plates with free edges and beams with a free end [5].. Next, using the discrete singular convolution (DSC) algorithm, they investigated the free vibration analysis of thin anisotropic and isotropic rectangular plates under various boundary conditions[6]. Based on Taylor’s series expansion, they proposed a unique scheme to apply for various boundary conditions.

Carrera *et.al* (2011) studied the vibration of anisotropic plates under simply supported boundary conditions by using Rayleigh-Ritz and variable kinematic method. They used a collection of

trigonometric functions and to demonstrate the accuracy of the results, convergence studies were made. They discussed the effects of the various factors including fiber orientation material, and the number of layers on the frequencies and mode shapes [7]. Eftekhari and Jafari (2012) combined the Ritz and differential quadrature (DQ) methods for the problem associated with the vibrations of the rectangular plate. As a result of this combination, they utilized both the simplicity of the Ritz method and the efficiency and high accuracy of the DQ method[8]. Eftekhari (2018) studied the free vibrations of both thick and thin rectangular plates under various boundary conditions using the coupled Ritz-finite element method [9]. Liu and Banerjee (2016) investigated the free vibrations of plates with arbitrary boundary conditions including rectangular cantilever plates using a novel spectral-dynamic stiffness method. The formulation, in a series sense, satisfies various boundary conditions, in addition to satisfying the governing differential equation exactly. Rui *et.al* (2018), using the rational superposition method in the symplectic space, obtained accurate analytical solutions applicable to the free vibration of rectangular cantilever plates. First, they constructed the Hamiltonian system-based governing equation. They demonstrated that the developed method leads to benchmark analytic solutions with satisfactory accuracy and fast convergence without assuming any trial solutions[10]. Xing *et.al* (2018), based on the Rayleigh quotient variational principle, developed a separation-of-variable method applicable to the free vibration analysis of rectangular thin plates. They developed an iterative separation-of-variable method which can be used for thin rectangular plates under various homogeneous boundary conditions. All closed-form solutions are presented in explicit forms, and using theoretical and numerical comparisons, validated the proposed methods and results [11]. Eisenberger and Deutsch studied the solution of a problem associated with the free vibrations of a thin rectangular plate with all combinations of boundary conditions including cantilever plates. They selected series that for various combinations of edge conditions, solve the partial differential equations of motion [12].

So far, only those studies related to the free vibrations of a low aspect ratio rectangular plate using the classical plate theory were mentioned. For the aeroelastic analysis of a rectangular cantilever plate, the beam theory is usually selected as the structural model [13-20]. The plate theories have been rarely used to model the structural response. As the flow is oriented along the wing's span direction the problem is called Flag-like configuration [21-24]. As the flow is oriented along the wing's chord direction the problem is called Wing-like configuration [25-27].

From the available vast literature for the free and forced vibrations of high and low aspect ratios of rectangular cantilever plates, one can see that the Rayleigh-Ritz method has been mainly applied, with the use of natural beam bending mode shapes. By considering the simplicity, the generality, and having less constraint in comparison with other solution techniques, the Rayleigh-Ritz method is preferred by many investigators.

In the present study, we will show how using some techniques in the Rayleigh-Ritz method leads to an improvement of the results and reduction of computational time significantly for the free vibration and consequently the aeroelastic analyses of a rectangular cantilever plate. For the structural and aeroelastic analyses in this study, the plate theory based on Kirchhoff hypothesis has been selected as the structural model. The Peter's theory is selected to model the aerodynamic loads on the plate due to the incompressible air flow. Using the Rayleigh-Ritz method the partial defferential equations are discretized. Various numbers of mode shapes have

been tried to prove the convergence of the results and the small perturbation flutter boundary is determined. The experimental data have been used to evaluate the theoretical results.

2. Mathematical model

2.1. Structural model

Various models have been adopted as a mathematical model to study the structural response of the rectangular plates. For a low aspect ratio, a thin plate classical plate theory is the first choice adopted by the researchers as the structural model. Fig. 1 presents a rectangular cantilever plate from the top view.

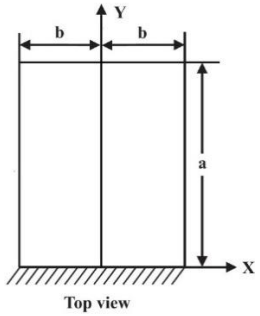

Fig 1: rectangular cantilever plate from the top view

According to the Kirchhoff hypothesis (1850), we assume that, before and after deformation, the cross-sections remain perpendicular to the mid–plane, without any kinds of warpings. Therefore, the shear deformation has been ignored.

As it can be seen in Fig. 1, a rectangular cantilever plate has been selected as the case study here. For an arbitrary point located on the plate element, the small displacements u_i are:

$$u_1 = U - z\frac{\partial W}{\partial x}, \qquad u_2 = V - z\frac{\partial W}{\partial y}, \qquad u_3 = W \tag{1}$$

where u_1, u_2, and u_3 are measured with respect to the xyz coordinate system and they are the displacement components of any point along x, y, and z axes, respectively. Also, U, V, and W which are measured with respect to the xyz coordinate system are the displacement components of the desired point on mid–plane. We noted that U, V, and W are independent of z.

By ignoring the in-plane motion $U = V = 0$

$$u_1 = -z\frac{\partial W(x,y,t)}{\partial x}, \qquad u_2 = -z\frac{\partial W(x,y,t)}{\partial y}, \qquad u_3 = W(x,y,t) \tag{2}$$

The total strain energy is

$$U = \frac{1}{2}\int (\sigma_{11}\epsilon_{11} + \sigma_{22}\epsilon_{22} + \sigma_{12}\epsilon_{12})dV \tag{3}$$

Using strain-displacements and stress-strain relationships Eq. (3) is written in the following form

$$U = \frac{1}{2}\int \left(\frac{E}{1-\nu^2}\left(-zW_{xx} - z\nu W_{yy}\right)^2 + \left(\frac{E}{1-\nu^2}\right)\left(\frac{1-\nu}{2}\right)\left(-z\nu W_{xx} - zW_{yy}\right)^2 + \left(\frac{E}{1-\nu^2}\right)\left(\frac{1-\nu}{2}\right)\left(-2zW_{xy}\right)^2\right)dV \tag{4}$$

By integrating with respect to z, one can write

$$U = \frac{D}{2}\int\int \left({W_{xx}}^2 + {W_{yy}}^2 + 2\nu W_{xx}W_{yy} + 2(1-\nu){W_{xy}}^2\right)dA \tag{5}$$

in which

$$D = \frac{Eh^3}{12(1-\nu^2)} \tag{6}$$

The following expression of the potential energy for the classical plate theory is more common in the literature

$$U = \frac{D}{2}\int\int \left(\left(\frac{\partial^2 W}{\partial^2 x} + \frac{\partial^2 W}{\partial^2 y}\right)^2 - 2(1-\nu)\left(\frac{\partial^2 W}{\partial^2 x}\frac{\partial^2 W}{\partial^2 y} - \left(\frac{\partial^2 W}{\partial x \partial y}\right)^2\right)\right)dA \tag{7}$$

For the classical plate theory, the kinetic energy is:

$$T = \frac{1}{2}\int\int \rho h\left(\frac{\partial W}{\partial t}\right)^2 dA \tag{8}$$

where h is the thickness of the palate. In the Rayleigh-Ritz method, W is approximated by the series as follows

$$W(x,y,t) = \sum_{i=1}^{M}\sum_{j=1}^{N} \phi_i(y)\psi_j(x)q_{ij}(t) \tag{9}$$

The best choice of ϕ_i and ψ_j could be made by using the mode functions of a free-free beam and cantilever beam as the admissible functions in the x and y directions of the cantilever plate, respectively. M and N are the number of the admissible functions in the y and x directions, respectively. We noted that for the x direction, two different trial functions have been considered in this study. First, the trial functions for a free-free beam which has been proposed and employed in [28] are considered. Second, a kind of polynomials is selected as the mode functions. We noted that the second type of mode functions has an important property and they

are compatible with the Peter's aerodynamic model. So, for the aeroelastic model, the second type has to be selected as the mode functions. The polynomials, $\zeta_j(x)$, are defined as follows[29]

$$\zeta_j(x) = \cos\big((j-1)\lambda\big) \quad and \quad \cos(\lambda) = \frac{x}{b} \tag{10}$$

So, it can be written

$$\begin{gathered}\zeta_1 = 1, \qquad \zeta_2 = \frac{x}{b}, \qquad \zeta_3 = 2\left(\frac{x}{b}\right)^2 - 1 \\ \zeta_4 = -3\left(\frac{x}{b}\right) + 4\left(\frac{x}{b}\right)^3, \qquad \dots\end{gathered} \tag{11}$$

Lagrange's equations for free vibrations are

$$\frac{d}{dt}\left(\frac{\partial L}{\partial \dot{q}_{ij}}\right) - \frac{\partial L}{\partial q_{ij}} + Q_{ij} = 0 \tag{12}$$

where

$$L = T - U, \qquad Q_{ij} = \iint p(x,y,t)\frac{\partial w}{\partial q_{ij}}\, dxdy \tag{13}$$

We noted that for the free vibrations, $Q_{ij} = 0$. Substituting Eq. (7) and Eq. (8) into Eq. (12) and Eq. (13), the final governing equations in matrix form to determine $q_{ij}(t)$ can be written as

$$[M]\{\ddot{q}_{ij}\} + [K]\{q_{ij}\} = 0 \tag{14}$$

2.2.Aerodynamic model

The Peters' model is selected to simulate the aerodynamic pressure on the case study considered here. We noted that the Peters' model provides moment and lift for each cross-section and therefore, can be only coupled with beam equations. So, to determine the pressure of the air flow on the plate, it is needed to make this aerodynamic model applicable to be combined with the plate theory. In the present study, Fourier transform has been employed to make Peters' model compatible with the classical plate theory.

Peters *et.al* introduces the generalized forces as follows [29]

$$L_n(x,t) = -\int_{-b}^{+b} \Delta P(x,y,t)cos(n\varphi)dy = -\int_0^{\pi} b\Delta P(x,y,t)cos(n\varphi)\sin\varphi\, d\varphi \tag{15}$$

in which, Δp is the pressure of the air flow on an arbitrary cross-section, and $n = 0, 1, 2, \dots$,

$$y = bcos(\varphi) \tag{16}$$

$L_n(x,t)$ can be written as follows:

$$L_n = -\int_0^{\pi} f(\varphi)cos(n\varphi)d\varphi \tag{17}$$

in which

$$f(\varphi) = b\Delta P \sin\varphi \tag{18}$$

By using the Fourier cosine series:

$$f(\phi) = a_0 + \sum_{n=1}^{\infty} a_n \cos\frac{n\pi\varphi}{L} \tag{19}$$

We put $L = \pi$. So we have

$$f(\phi) = a_0 + \sum_{n=1}^{\infty} a_n \cos n\varphi \tag{20}$$

in which

$$a_0 = \frac{1}{\pi}\int_0^{\pi} f(\varphi)d\varphi \quad and \quad a_n = \frac{2}{\pi}\int_0^{\pi} f(\varphi)cos(n\varphi)d\varphi \ , n = 1, 2, 3, \dots \tag{21}$$

From Eqs. (17) and (21), we can write:

$$a_0 = -\frac{L_0}{\pi} \qquad and \qquad a_n = -\frac{2L_n}{\pi} \tag{22}$$

Therefore

$$f(\varphi) = b\Delta P \sin\varphi = -\frac{L_0}{\pi} - \frac{2L_1}{\pi}\cos\varphi - \frac{2L_2}{\pi}\cos 2\varphi + \cdots \tag{23}$$

Finally, the pressure distribution is written as follows:

$$p(x,y,t) = \Delta P = -\frac{L_0(x,t)}{\pi b \sin\varphi} - \frac{2L_1(x,t)}{\pi b \sin\varphi}\cos\varphi - \frac{2L_2(x,t)}{\pi b \sin\varphi}\cos 2\varphi - \frac{2L_3(x,t)}{\pi b \sin\phi}\cos 3\phi + \cdots \tag{24}$$

In Eq (24), L_0, L_1, L_2, etc. can be written by using lateral displacement of the plate in z direction. Therefore, ΔP can be approximated using an arbitrary number of L_n. We noted that in the Rayleigh-Ritz method, the number of mode functions in the y direction should be equal to the number of L_n. For instance, if L_0, L_1, and L_2 are considered in the ΔP, the functions $\zeta_1 = 1$, $\zeta_2 = \frac{x}{b}$, and $\zeta_3 = 2\left(\frac{x}{b}\right)^2 - 1$ have to be selected in the Rayleigh-Ritz method. So, ΔP can be approximated using an arbitrary number of L_n.

2.3.Aeroelastic Model

Using the Eqs. (24) and Eq. (13), we can determine Q_{ij} in its' final form. Also, by using Eqs (7), (8), and (13), the final forms of $\frac{d}{dt}\left(\frac{\partial L}{\partial \dot{q}_{ij}}\right)$ and $\frac{\partial L}{\partial q_{ij}}$ can be expressed. Finally, the terms $\frac{d}{dt}\left(\frac{\partial L}{\partial \dot{q}_{ij}}\right)$, $\frac{\partial L}{\partial q_{ij}}$, and Q_{ij} are replaced into Eq. (12), and therefore, the final matrix form equations governing the aeroelastic system is derived. Using a simple series of mathematical operations, The final matrix form of equations is written as follows

$$[\mathbf{A}]\{\dot{x}\} + [\mathbf{B}]\{x\} = 0 \tag{25}$$

which is applicable for the eigenvalue problem and consequently performing the flutter analysis. We noted $\{x\}$, in Eq (25) are the time-dependent state variables of the aeroelastic system.

3. Results

In the present study, we divided the results section into two main parts. First, the results of the free vibration analysis have been presented. A cantilever plate with variable width is considered here as a case study. First, the convergence test using a different number of mode shapes in each direction has been done. Next, the theoretical results have been compared with published as well as previously unpublished data obtained from an experiment carried out at Duke University. After the presentation of the results obtained from the structural analysis, the results associated with the aeroelastic analysis of a rectangular cantilever plate will be presented. The experimental data published in [25] as well as previously unpublished data have been used to evaluate the theoretical results. It has been shown that using some techniques in the Rayleigh-Ritz method can lead to an improvement of both free vibrations and aeroelastic results. An aluminium alloy plate is selected as the case study which Table 1 shows its' parameters.

Table 1. Properties of the plate

Length	275 mm
Width	151, 108, 55 mm
Thickness	0.381 mm
Density	2840 kg/m3
Young's modulus	72 GPa
Poisson's ratio	0.3

3.1.The free vibrations analysis

3.1.1Convergence test

Table 2 presents the convergence test for the 275 mm × 151 mm rectangular cantilever plate using beam characteristic functions in both x and y directions. In other words, mode shapes for a free–free beam and cantilever beam are adopted as the mode functions in the x and y directions, respectively. The theoretical natural frequencies are determined by solving Eq. (25), ignoring the aerodynamic forces.

Table 2. Convergence test for 275 mm × 151 mm rectangular plate using mode functions for cantilever beam and free–free beam as the admissible functions in the y and x directions, respectively

Frequency (Hz)	$M \times N$						
	3×1	4×1	5×1	5×2	5×3	5×4	5×5
First Bending	4.2536	4.2536	4.2536	4.2536	4.2536	4.2536	4.2536
First Torsion	-	-	-	16.6120	16.6120	16.5928	16.5928
Second Bending	26.6572	26.6572	26.6572	26.6572	26.6572	26.6572	26.6572
Second Torsion	-	-	-	55.1597	55.1597	54.8352	54.8352
Third Bending	74.6409	74.6409	74.6409	74.6409	74.6409	74.6409	74.6409

From Table 2, we can see that the torsional frequencies change only when N increases from an odd number to an even number. It means that when we increase the number of admissible functions in x direction from an even number such as 2 to an odd number, such as 3, the torsional frequencies remained unchanged. For more investigation, we try another kind of admissible function in x direction.

Table 3 indicates the convergence test for the 275 mm × 151 mm rectangular cantilever plate using mode functions for a cantilever beam in the y direction and polynomials defined earlier in the x direction. N is the number of admissible functions in the x direction and similarly, M is the number of structural mode shapes in the y direction.

Table 3. Convergence test for 275 mm × 151 mm rectangular plate using mode functions for a cantilever beam in the y direction and polynomials in chord-direction

Frequency (Hz)	$M \times N$						
	3×1	4×1	5×1	5×2	5×3	5×4	5×5
First Bending	4.2956	4.2956	4.2956	4.2956	4.2956	4.2956	4.2956
First Torsion	-	-	-	16.7767	16.7767	16.7814	16.7814
Second Bending	26.9202	26.9202	26.9202	26.9202	26.9202	26.9202	26.9202
Second Torsion	-	-	-	55.7200	55.7200	55.7054	55.7054
Third Bending	75.3773	75.3773	75.3773	75.3773	75.3773	75.3773	75.3773

From the tables above, it can be seen that considering two and three mode shapes in the x and y directions, respectively, ($N = 2$ and $M = 3$) is sufficiently well to capture the first five natural frequencies of a rectangular plate with an aspect ratio above $\frac{275}{151} \approx 1.8$.

From both tables 2 and 3, we can see that the torsional frequencies change only when N increases from 3 to 4. In other words, the torsional frequencies change only when N increases from an odd number to an even number. It means that when N is increased, for example, from 2 to 3, no anti-symmetric mode function is added to the Eq. (9). So, it can be concluded that the

symmetric and anti-symmetric mode functions in the x direction are completely decoupled from each other. This finding enables us to use different kinds of admissible functions in the y direction for symmetric and anti-symmetric mode functions. In this regard, we consider the bending modes of a uniform cantilever beam as an admissible function for the symmetric mode of the cantilever plate and the torsional modes of a uniform cantilever beam as an admissible function for the anti-symmetric mode of the cantilever plate, both in the y direction. To express this technique clearly, first, we rewrite Eq.9 in the following form:

$$w(x,y,t) = \sum_{i=1}^{M} \phi_i(y)\psi_1(x)q_{i1}(t) + \sum_{i=1}^{M} \phi_i(y)\psi_2(x)q_{i2}(t) + \sum_{i=1}^{M} \phi_i(y)\psi_3(x)q_{i3}(t) + \cdots \quad (26)$$

We noted that $\psi_1(x)$, $\psi_3(x)$, $\psi_5(x)$, etc. are even functions or symmetric mode functions and $\psi_2(x)$, $\psi_4(x)$, $\psi_6(x)$, etc. are odd functions or anti-symmetric mode functions. According to the technique mentioned above, Eq. 26 can be written as follow.

$$w(x,y,t) = \sum_{i=1}^{M} \phi_i(y)\psi_1(x)q_{i1}(t) + \sum_{i=1}^{M} \theta_i(y)\psi_2(x)q_{i2}(t) + \sum_{i=1}^{M} \phi_i(y)\psi_3(x)q_{i3}(t) + \cdots \quad (27)$$

As it can be seen in Eq. 27, the bending mode shapes $\phi_i(y)$ have been replaced by the torsional mode shapes $\theta_i(y)$ in series contain anti-symmetric mode functions. In addition, by using this technique in the Rayleigh-Ritz method, two sets of completely decoupled equations will be formed. In other words, the number of equations of the plate is divided into two different sets. One set is the equations governing the symmetric modes and another includes equations governing the anti-symmetric modes. In this way, the total number of equations of the cantilever plate which have to be solved simultaneously is divided by two. Therefore, the computational time needed for the solution of the equations is reduced significantly. This could be also an asset in circumstances when we have a constraint in choosing the admissible functions for the Rayleigh-Ritz method. In cases, when the quality of the admissible functions for the rectangular cantilever plate is not as well as beam characteristic functions, which according to the literature is the best choice for the Rayleigh-Ritz method, it is needed to increase the number of mode functions to compensate for the quality of the admissible functions. This action ends up increasing the computational the time significantly. However, using the technique mentioned above lead to a reduction of time needed to solve the equations considerably. In the next part, by using the experimental data the evaluation of the mentioned technique is done.

3.1.2.Comparison between the theory and experiment

In this part, comparisons are made between theory and experiment. The experimental data obtained at Duke University including those published in [25] as well as previously unpublished data. The out of plane motions of the rectangular cantilever plate has been estimated by the Rayleigh-Ritz method. However, we should note that in this method the modes of the plate have been divided into two different sets. I: symmetric modes and II: Anti-symmetric modes. First, we use bending mode functions of a uniform cantilever beam for both the symmetric and anti-symmetric mode functions. In the next step, we consider the torsional and bending mode

functions of a uniform cantilever beam for the anti-symmetric and symmetric mode functions, respectively.

As we mentioned above, using the form of distribution mentioned in Eq. 26 provides differential equations governing symmetric and anti-symmetric mode shapes, separately. This separation enables us to use different mode shapes along the x axis for symmetric and anti-symmetric mode shapes. Table 4 presents how the torsional frequency is affected by using various types of mode shapes. We noted that considering the torsional mode functions of a uniform cantilever beam for the anti-symmetric mode functions, does not affect the bending frequencies. Therefore, we have only discussed how various types of mode shapes affect the torsional frequency.

Table 4. The effect of the mode shapes on Torsional frequency

	Frequency (Hz)					
Dimensions	275 mm × 151 mm		275 mm × 108 mm		275 mm × 55 mm	
Trial Functions	First Torsion	Second Torsion	First Torsion	Second Torsion	First Torsion	Second Torsion
Bending–Bending modes (BB)	16.6120	55.1597	22.1618	70.8790	41.7057	127.6858
Bending– Torsional modes (BT)	14.4960	50.3267	20.0566	65.2839	39.4449	121.0679
Experimental (EX)	18.56	58.63	23.41	70.87	38.43	119.3
Percent Difference (between BB and EX)	10.5	6	5.5	≈ 0	8.5	7
Percent Difference (between BT and EX)	22	14	14.5	8	2.5	1.5

As it can be seen from Table 4, for the rectangular cantilever plates of dimensions 275 mm × 151 mm and 275 mm × 108 mm the use of bending mode shapes of a uniform cantilever beam for both the anti-symmetric and symmetric modes lead to natural frequencies closer to the experimental values. The most compatible results of the use of bending mode shapes of a uniform cantilever beam for both the anti-symmetric and symmetric modes are for the plate with dimensions 275 mm × 108 mm. For a cantilever plate with an aspect ratio of $AR = 275/55 = 5$, using bending mode shapes of a uniform cantilever beam for both the anti-symmetric and symmetric modes leads to upper bound values for the natural torsional frequencies as compared to the experimental values. While, for a cantilever plate with an aspect ratio of $AR = 275/151 \approx 1.8$, using bending mode shapes of a uniform cantilever beam for both the anti-symmetric and symmetric modes leads to lower bound values for the natural torsional frequencies as compared to the experimental values. So, it can be concluded that when the aspect ratio is increased from 1.8 to 2.5, the accuracy of the theory with the use of bending mode shapes is increasing. While, by the increase of the aspect ratio from 2.5 to 5, the distance between the experimental values and results obtained from the theory with the use of bending mode shapes is becoming larger. It is apparent from this table that for a cantilever plate with aspect ratios 5, the approximation of anti-symmetric mode shapes by the natural beam torsional mode shapes significantly improves the accuracy of predicted natural torsional frequencies.

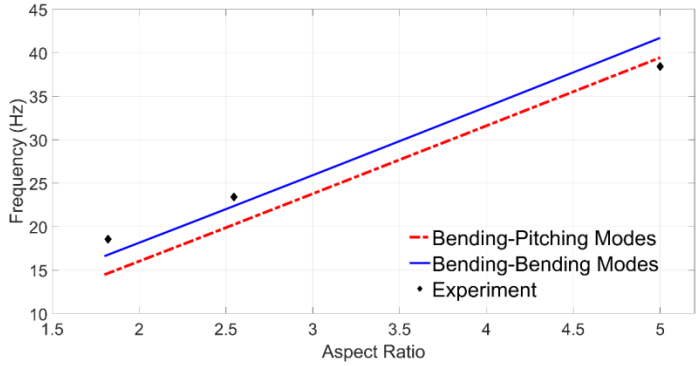

(a) First torsional frequency

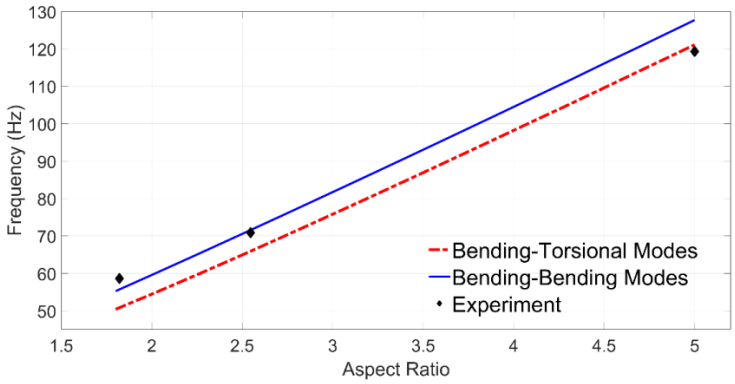

(b) Second torsional frequency

Fig 2: Experimental vs. theoretical torsional natural frequencies.

Fig. 2 shows the theoretical versus experimental torsional natural frequencies for the three plates considered in this study. There is good agreement between both theories and the experiment in trend. However, as we noted earlier, for lower aspect ratios, the results obtained from the use of bending mode shapes of a uniform cantilever beam for both the anti-symmetric and symmetric modes are more compatible with the experimental data in magnitude. By the increase of the aspect ratio, the approximation of anti-symmetric mode shapes by the natural beam torsional mode shapes leads to the natural torsional frequencies closer to the experimental data.

3.2.The aeroelastic analysis

So far, the free vibrations response of a cantilever plate obtained from using different types of admissible functions in the Rayleigh-Ritz method is discussed. It was shown that for a cantilever plate with aspect ratios 5, using the natural beam torsional mode shapes for the approximation of anti-symmetric modes, significantly improves the accuracy of predicted natural torsional frequencies. Also, we know that the aeroelastic flutter of a rectangular cantilever plate is the bending-torsion type. Therefore, it is predicted that the first torsional and bending modes to be

effective factors for determining the speed of flutter. Therefore, it would be desired to investigate the impact of using different kinds of admissible functions for both the anti-symmetric and symmetric modes on the aeroelastic response of a rectangular cantilever plate. Therefore, the speed of flutter for a plate of an aspect ratio 5, has been determined theoretically and compared with the experiment.

Figures 3 presents the aeroelastic damping with respect to flow velocity using bending mode shapes of a uniform cantilever beam for both the anti-symmetric and symmetric modes and compares with the results derived from the use of the natural beam torsional mode shapes for anti-symmetric modes. Figure 3 contains the real component of the eigenvalue plotted versus the flow velocity. In other words, the damping value in Figure 3 is the real part of the characteristic equation's roots of the aeroelastic system. The form of the characteristic equation's roots of the aeroelastic system, same as the characteristic equation's roots of the ordinary mass spring damper system, is $\xi\omega_n \pm i\sqrt{1-\xi^2}\,\omega_n$. ξ is dimensionless and the dimension of ω_n is one per second. So the dimension of the damping is one per second. Figure 3 reveals that for a cantilever plate with a moderate aspect ratio (aspect ratio around 5), the approximation of anti-symmetric modes by the natural beam torsional mode shapes increases the compatibility between the theoretical and experimental results, in comparison to the use of bending mode shapes of a uniform cantilever beam for both the anti-symmetric and symmetric modes. In addition, it can be seen from Fig. 3, that using bending mode shapes for both the anti-symmetric and symmetric modes leads to upper flutter speed. This can be explained by the fact that using bending mode shapes for both the anti-symmetric and symmetric modes, causes higher torsional stiffness and consequently higher torsional frequencies. The higher torsional stiffness can delay the flutter boundary of the structure.

Table 5 presents the speed of flutter for a 275 mm × 55 mm cantilever plate derived from the plate theory by using different kinds of mode shapes and compares the results to the experimental data. The speed of flutter obtained by using the beam torsional mode shapes is much closer to the experimental values. The percent difference for the flutter speed between the result obtained from the use of bending mode shapes of a uniform cantilever beam for both the anti-symmetric and symmetric modes and the experimental value is 24 percent. The approximation of anti-symmetric modes by the natural beam torsional mode shapes leads to a significant reduction of the difference to the value of 8 percent.

From Table 4, we can see that there is an 8 percent difference between the first torsional frequency obtained from the use of bending mode shapes of a uniform cantilever beam for both the symmetric and anti-symmetric modes and the experiment. The use of torsional mode shapes of a uniform cantilever beam for the anti-symmetric modes reduces the difference between the theory and experiment to 2.5 percent. By comparison the difference between theoretical and experimental data in both the free vibrations and aeroelastic analyses, it can be concluded that the difference in structural models leads to a more significant difference in the aeroelastic response. 2.5 and 8 present differences in the structural models end up having 8 and 24 present differences in the aeroelastic models. Therefore, selecting an appropriate admissible function to approximate the structural response of a rectangular cantilever plate is of great importance.

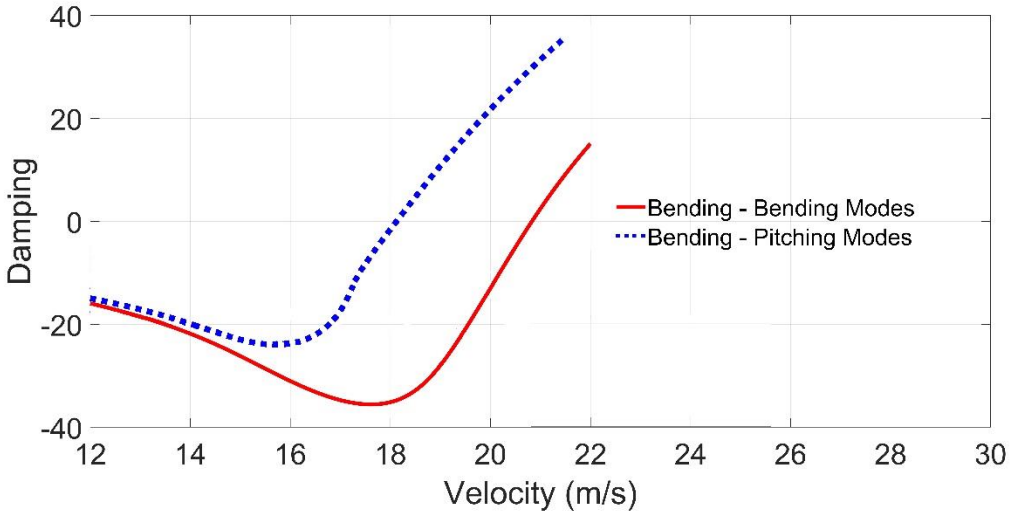

Fig 3: Damping with respect to velocity using different kinds of mode shapes

Table 5: The speed of flutter for a 275 mm × 55 mm rectangular plate

	Bending-Torsional Modes	**Bending-Bending Modes**	**Experimental Result**
Flutter Speed (m/s)	18.1	20.9	16.7

4. Conclusion

In the present study, the free vibrations and aeroelastic problems of rectangular cantilever plates with varying aspect ratio have been investigated by using the classical plate theory based on the Kirchhoff hypothesis. The Peter's theory is selected to model the aerodynamic pressure on the plate due to the incompressible air flow. To discretize the partial differential equations of the system, the Rayleigh-Ritz method has been applied and by using Lagrange equations, the mass, damping, and stiffness matrices have been derived. Various numbers of mode shapes are used to show the convergence of the system's response. The theoretical results including the natural frequencies and flutter speed have been evaluated by using the experimental data. A summary of the results is as follows:

The convergence test using a different number of mode shapes in each direction proved that taking two modes in the chord direction is sufficient to determine the first five natural frequencies of a cantilever plate with an aspect ratio above $AR = 1.8$

The final equations obtained from the classical plate theory can be divided into two sets of decoupled equations governing symmetry and anti-symmetry mode functions. This separation enables us to use different mode shapes along the x axis for symmetry and anti-symmetry mode functions. For a cantilever plate with a moderate aspect ratio (aspect ratio around 5), the approximation of anti-symmetric mode shapes by the natural beam torsional mode shapes

significantly improves the accuracy of predicted natural torsional frequencies. It should be noted that this change does not have any effects on the natural bending frequency. Furthermore, as a result of two decoupled set of equations, the number of equations which have to be solved simultaneously is divided by two. This could lead to a reduction of computational time by one-fifth. For my case study and with my system, when $M = N = 5$, the computational time decreased from 960 seconds to 166 seconds.

For a cantilever plate with aspect ratio $AR = 1.8$, using bending mode shapes of a uniform cantilever beam for both the anti-symmetric and symmetric modes leads to lower bound values for the natural torsional frequencies as compared to the experimental values. While, For a cantilever plate with aspect ratio $AR = 5$, using bending mode shapes of a uniform cantilever beam for both the anti-symmetric and symmetric modes leads to upper bound values for the natural torsional frequencies as compared to the experimental values.

With the increase of the aspect ratio from 1.8 to 2.5, the accuracy of the theory with the use of bending mode shapes is increasing. While, by increasing the aspect ratio from 2.5 to 5, the distance between the experimental values and results obtained from the theory with the use of bending mode shapes is becoming larger.

For a cantilever plate with a moderate aspect ratio, the approximation of anti-symmetric modes by the natural beam torsional mode shapes leads to the theoretical results closer to the experiment, in comparison to the use of bending mode shapes of a uniform cantilever beam for both the anti-symmetric and symmetric modes.

By comparison the difference between theoretical and experimental data in both the free vibrations and aeroelastic analyses, it can be concluded that the difference in structural models leads to a more significant difference in the aeroelastic response. 2.5 and 8 present differences in the structural models end up having 8 and 24 present differences in the aeroelastic models. Therefore, selecting an appropriate admissible function to approximate the structural response of a rectangular cantilever plate is of great importance.

Using bending mode shapes for both the anti-symmetric and symmetric modes causes higher torsional stiffness and consequently higher torsional frequencies. The higher torsional stiffness can delay the flutter boundary of the structure.

References

[1] A.W. Leissa, Vibration of plates, Scientific and Technical Information Division, National Aeronautics and …, 1969.
[2] H.-S. Shen, Y. Chen, J. Yang, Bending and vibration characteristics of a strengthened plate under various boundary conditions, Engineering structures, 25 (2003) 1157-1168.
[3] J. Seok, H.F. Tiersten, H.A. Scarton, Free vibrations of rectangular cantilever plates. Part 1: out-of-plane motion, Journal of sound and vibration, 271 (2004) 131-146.
[4] J. Seok, H.F. Tiersten, H.A. Scarton, Free vibrations of rectangular cantilever plates. Part 2: in-plane motion, Journal of sound and vibration, 271 (2004) 147-158.
[5] X. Wang, S. Xu, Free vibration analysis of beams and rectangular plates with free edges by the discrete singular convolution, Journal of Sound and Vibration, 329 (2010) 1780-1792.
[6] Q. Zhu, X. Wang, Free vibration analysis of thin isotropic and anisotropic rectangular plates by the discrete singular convolution algorithm, International Journal for Numerical Methods in Engineering, 86 (2011) 782-800.
[7] E. Carrera, F.A. Fazzolari, L. Demasi, Vibration analysis of anisotropic simply supported plates by using variable kinematic and Rayleigh-Ritz method, Journal of vibration and acoustics, 133 (2011).

[8] S.A. Eftekhari, A.A. Jafari, A mixed method for free and forced vibration of rectangular plates, Applied Mathematical Modelling, 36 (2012) 2814-2831.
[9] S.A. Eftekhari, A coupled ritz-finite element method for free vibration of rectangular thin and thick plates with general boundary conditions, Steel and Composite Structures, 28 (2018) 655-670.
[10] R. Li, P. Wang, Z. Yang, J. Yang, L. Tong, On new analytic free vibration solutions of rectangular thin cantilever plates in the symplectic space, Applied Mathematical Modelling, 53 (2018) 310-318.
[11] Y. Xing, Q. Sun, B.o. Liu, Z. Wang, The overall assessment of closed-form solution methods for free vibrations of rectangular thin plates, International Journal of Mechanical Sciences, 140 (2018) 455-470.
[12] M. Eisenberger, A. Deutsch, Solution of thin rectangular plate vibrations for all combinations of boundary conditions, Journal of Sound and Vibration, 452 (2019) 1-12.
[13] M. Goland, The flutter of a uniform cantilever wing, Journal of Applied Mechanics-Transactions of the Asme, 12 (1945) A197-A208.
[14] M.J. Patil, D.H. Hodges, C.E.S. Cesnik, Characterizing the effects of geometrical nonlinearities on aeroelastic behavior of high-aspect ratio wings, in: NASA Conference Publication, NASA, 1999, pp. 501-510.
[15] M.J. Patil, D.H. Hodges, On the importance of aerodynamic and structural geometrical nonlinearities in aeroelastic behavior of high-aspect-ratio wings, Journal of Fluids and Structures, 19 (2004) 905-915.
[16] M.J. Patil, D.H. Hodges, C.E.S. Cesnik, Limit-cycle oscillations in high-aspect-ratio wings, Journal of fluids and structures, 15 (2001) 107-132.
[17] D. Tang, E.H. Dowell, Experimental and theoretical study on aeroelastic response of high-aspect-ratio wings, AIAA journal, 39 (2001) 1430-1441.
[18] D.M. Tang, E.H. Dowell, Effects of geometric structural nonlinearity on flutter and limit cycle oscillations of high-aspect-ratio wings, Journal of fluids and structures, 19 (2004) 291-306.
[19] D. Tang, E.H. Dowell, Experimental and theoretical study of gust response for high-aspect-ratio wing, AIAA journal, 40 (2002) 419-429.
[20] A.H. Modaress-Aval, F. Bakhtiari-Nejad, E.H. Dowell, D.A. Peters, H. Shahverdi, A comparative study of nonlinear aeroelastic models for high aspect ratio wings, Journal of Fluids and Structures, 85 (2019) 249-274.
[21] W. Zhao, M.P. Païdoussis, L. Tang, M. Liu, J. Jiang, Theoretical and experimental investigations of the dynamics of cantilevered flexible plates subjected to axial flow, Journal of Sound and Vibration, 331 (2012) 575-587.
[22] S.C. Gibbs, I. Wang, E. Dowell, Theory and experiment for flutter of a rectangular plate with a fixed leading edge in three-dimensional axial flow, Journal of Fluids and Structures, 34 (2012) 68-83.
[23] M. Colera, M. Pérez-Saborid, Numerical investigation of the effects of compressibility on the flutter of a cantilevered plate in an inviscid, subsonic, open flow, Journal of Sound and Vibration, 423 (2018) 442-458.
[24] A.H. Modaress-Aval, F. Bakhtiari-Nejad, E.H. Dowell, H. Shahverdi, H. Rostami, D.A. Peters, Aeroelastic analysis of cantilever plates using Peters' aerodynamic model, and the influence of choosing beam or plate theories as the structural model, Journal of Fluids and Structures, 96 (2020) 103010.
[25] S.C. Gibbs, A. Sethna, I. Wang, D. Tang, E.H. Dowell, Aeroelastic stability of a cantilevered plate in yawed subsonic flow, Journal of Fluids and Structures, 49 (2014) 450-462.
[26] S.C. Gibbs IV, I. Wang, E.H. Dowell, Stability of rectangular plates in subsonic flow with various boundary conditions, Journal of Aircraft, 52 (2015) 439-451.
[27] T. Chen, M. Xu, D. Xie, X. An, Post-flutter response of a flexible cantilever plate in low subsonic flows, International Journal of Non-Linear Mechanics, 91 (2017) 113-127.
[28] E.H. Dowell, On asymptotic approximations to beam modal functions, Journal of Applied Mechanics, 51 (1984) 439.
[29] D.A. Peters, M.c.A. Hsieh, A. Torrero, A State-Space Airloads Theory for Flexible Airfoils, Journal of the American Helicopter Society, 52 (2007) 329-342.